

See discussions, stats, and author profiles for this publication at: <https://www.researchgate.net/publication/32136965>

Three-Dimensional Observation of Phase-Separated Silica-Based Gels Confined between Parallel Plates

ARTICLE *in* LANGMUIR · JULY 2003

Impact Factor: 4.46 · DOI: 10.1021/la026715s · Source: OAI

CITATIONS

32

READS

16

4 AUTHORS, INCLUDING:



Kazuki Nakanishi

Kyoto University

359 PUBLICATIONS 11,704 CITATIONS

SEE PROFILE



Hiroshi Jinnai

Tohoku University

234 PUBLICATIONS 4,217 CITATIONS

SEE PROFILE

Three-Dimensional Observation of Phase-Separated Silica-Based Gels Confined between Parallel Plates

Kazuyoshi Kanamori,* Kazuki Nakanishi,† Kazuyuki Hirao, and Hiroshi Jinnai‡

Department of Material Chemistry, Graduate School of Engineering, Kyoto University,
Yoshida Sakyo-ku, Kyoto 606-8501, Japan

Received October 18, 2002. In Final Form: February 13, 2003

Methyl-siloxane gel and silica gel with co-continuous structure derived from methyltrimethoxysilane (MTMS) and tetramethoxysilane (TMOS) were synthesized in two-dimensional (2D) confined spaces by inducing spinodal decomposition during the sol–gel transition. The resultant macroporous gel morphology was three-dimensionally examined by laser scanning confocal microscopy (LSCM), which revealed that the 2D confined gels have a layered structure. At the interface between MTMS- or TMOS-derived gel and a hydrophobic surface, the skin layer has formed by complete wetting by methylsiloxane and silica phase. In the near-surface region, a cylindrical columnar gel skeleton has formed only in the MTMS system. The volume fraction of gel phase oscillated near both hydrophobic and hydrophilic surfaces because of the attractive interactions between polymerizing siloxane and surfaces or shrinkage during aging stage.

1. Introduction

It is known that well-defined macroporous silica-based gels with co-continuous structure can be prepared by inducing spinodal decomposition during the sol–gel transition.^{1–3} In a system containing formamide as a polar solvent, tetramethoxysilane (TMOS) or methyltrimethoxysilane (MTMS) as a silica source, and nitric acid as an acid catalyst, phase separation occurs between the polar solvent and the polymerizing siloxane component.⁴ The co-continuous silica gel has found an application as a separation medium for high-performance liquid chromatography (HPLC),^{5,6} and the miniaturization of the separation medium is of high technical interest.^{7–12} In applying such continuous porous material to microdevices such as capillary columns, thin-layer chromatography plates, and chip columns, the surface effect cannot be neglected. Namely, in such a microconfined space, since the ratio of surface area to total volume of a sample becomes larger, wetting phenomena and shrinkage during

aging and drying process will presumably change the morphogenesis and phase-separation tendency.

In the phase-separating polymer blends in confined geometry, preferential wetting of surfaces by one component strongly influences the phase-separation behavior;^{13–20} this wetting phenomenon induces the so-called “surface-directed spinodal decomposition” in the early stage of spinodal decomposition and it finally brings the system into a layered structure stacked perpendicular to the surface.^{21–33} The influence of this spinodal decomposition perpendicular to the surface increases with decreasing film thickness because the part of the film that is in close proximity to the surfaces amounts to a significant portion of the total volume of the system. Another effect that becomes significant when thickness of the film decreases is surface-induced spinodal waves from both sides of the film that interfere with each other, so the

* To whom correspondence should be addressed. E-mail: kazuki@bisco1.kuic.kyoto-u.ac.jp.

† Structural Ordering and Physical Properties, PRESTO, JST, Japan. (Kazuki Nakanishi has double affiliations.)

‡ Department of Polymer Science and Engineering, Kyoto Institute of Technology, Matsugasaki, Sakyo-ku, Kyoto 606-8585, Japan.

- (1) Nakanishi, K. *J. Porous Mater.* **1997**, *4*, 67.
- (2) Nakanishi, K.; Takahashi, R.; Nagakane, T.; Kitayama, K.; Koheiya, N.; Shikata, H.; Soga, N. *J. Sol-Gel Sci. Tech.* **2000**, *17*, 191.
- (3) Nakanishi, K. *J. Sol-Gel Sci. Tech.* **2000**, *19*, 65.
- (4) Kaji, H.; Nakanishi, K.; Soga, N. *J. Sol-Gel Sci. Tech.* **1993**, *1*, 35.
- (5) Tanaka, N.; Kobayashi, H.; Nakanishi, K.; Minakuchi, H.; Ishizuka, N. *Anal. Chem.* **2001**, *73*, 420A.
- (6) Tanaka, N.; Kobayashi, H.; Ishizuka, N.; Minakuchi, H.; Nakanishi, K.; Hosoya, K.; Ikegami, T. *J. Chromatogr. A*, in press.
- (7) Ishizuka, N.; Minakuchi, H.; Nakanishi, K.; Soga, N.; Hosoya, K.; Tanaka, N. *J. High Resolut. Chromatogr.* **1998**, *21*, 477.
- (8) Tanaka, N.; Nagayama, H.; Kobayashi, H.; Ikegami, T.; Hosoya, K.; Ishizuka, N.; Minakuchi, H.; Nakanishi, K.; Cabrera, K.; Lubda, D. *J. High Resolut. Chromatogr.* **2000**, *23*, 111.
- (9) Ishizuka, N.; Minakuchi, H.; Nakanishi, K.; Soga, N.; Nagayama, H.; Hosoya, K.; Tanaka, N. *Anal. Chem.* **2000**, *72*, 1275.
- (10) Ishizuka, N.; Minakuchi, H.; Nakanishi, K.; Hirao, K.; Tanaka, N. *J. Sol-Gel Sci. Tech.* **2000**, *19*, 371.
- (11) Kumon, S.; Nakanishi, K.; Hirao, K. *J. Sol-Gel Sci. Tech.* **2000**, *19*, 553.
- (12) Nakanishi, K.; Kumon, S.; Hirao, K.; Jinnai, H. *Mater. Res. Soc. Symp. Proc.* **2000**, *628*, CC7.6.1.

- (13) Steiner, U.; Klein, J.; Eiser, E.; Budkowski, A.; Fetters, L. J. *Science* **1992**, *258*, 1126.
- (14) Tanaka, H. *Pys. Rev. Lett.* **1993**, *70*, 53.
- (15) Tanaka, H. *Pys. Rev. Lett.* **1993**, *70*, 2770.
- (16) Tanaka, H. *Europhys. Lett.* **1993**, *24*, 665.
- (17) Puri, S.; Binder, K. *Phys. Rev. E* **1994**, *49*, 5359.
- (18) Tanaka, H.; Sigehuzi, T. *Phys. Rev. Lett.* **1995**, *52*, 829.
- (19) Rysz, J.; Budkowski, A.; Bernasik, A.; Klein, J.; Kowalski, K.; Jedliński, J.; Fetters, L. J. *Europhys. Lett.* **2000**, *50*, 35.
- (20) Tanaka, H. *J. Phys.: Condens. Matter* **2001**, *13*, 4637.
- (21) Jones, R. A. L.; Norton, L. J.; Kramer, E. J.; Bates, F. S.; Wiltzius, P. *Phys. Rev. Lett.* **1991**, *66*, 1326.
- (22) Bruder, F.; Brenn, R. *Phys. Rev. Lett.* **1992**, *69*, 624.
- (23) Budkowski, A.; Steiner, U.; Klein, J. *J. Chem. Phys.* **1992**, *97*, 5229.
- (24) Hariharan, A.; Kumar, S. K.; Rafailovich, M. H.; Sokolov, J.; Zheng, X.; Duong, D.; Schwarz, S. A.; Russell, T. P. *J. Chem. Phys.* **1993**, *99*, 656.
- (25) Krausch, G.; Dai, C.; Kramer, E. J.; Bates, F. S. *Phys. Rev. Lett.* **1993**, *71*, 3669.
- (26) Marko, J. F. *Phys. Rev. E* **1993**, *48*, 2861.
- (27) Krausch, G. *Mater. Sci. Eng. Rep.* **1995**, *R14*, 1.
- (28) Geoghegan, M.; Jones, R. A. L.; Clough, A. S. *J. Chem. Phys.* **1995**, *103*, 2719.
- (29) Rysz, J.; Bernasik, A.; Ermer, H.; Budkowski, A.; Brenn, R.; Hashimoto, T.; Jedliński, J. *Europhys. Lett.* **1997**, *40*, 503.
- (30) Cherrabi, R.; Saout-Elhak, A.; Benhamou, M. *J. Chem. Phys.* **1999**, *111*, 8174.
- (31) Rysz, J.; Ermer, H.; Budkowski, A.; Lekka, M.; Bernasik, A.; Wróbel, S.; Brenn, R.; Lekki, J.; Jedliński, J. *Vacuum* **1999**, *54*, 303.
- (32) Bernasik, A.; Rysz, J.; Budkowski, A.; Kowalski, K.; Camra, J.; Jedliński, J. *Macromol. Rapid Commun.* **2001**, *22*, 829.
- (33) Morita, H.; Kawakatsu, T.; Doi, M. *Macromolecules* **2001**, *34*, 8777.

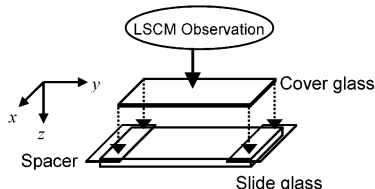


Figure 1. Schematic illustration of the 2D mold for gel preparation, axis definition, and the observation direction of LSCM.

intriguing morphology perpendicular to the surfaces appears.³⁴ These phenomena are of great importance in designing thin polymer films. Specifically, in the phase-separated alkylsilicate sol–gel system confined between two substrates, structural inhomogeneity has been observed perpendicular to the surface.³⁵

Recently, real-space analysis techniques of phase-separated polymer mixtures have been developed utilizing laser scanning confocal microscopy (LSCM).^{36–38} By using LSCM, optically sliced two-dimensional images along the incident beam can be obtained. The series of sliced images is appropriately digitized and reconstructed to perform the 3D analyses. A bulk-sintered silica gel with co-continuous structure has already been successfully analyzed three-dimensionally by this method; it is revealed that the geometrical features of the co-continuous silica gel are comparable to a phase-separating polymer blend at a similar volume fraction.³⁹

In the present study, silica-based gels with co-continuous structure were prepared by the method in two-dimensionally confined space such as a gap between two parallel plates, and the structural variety of confined gels was three-dimensionally observed by LSCM. The variety of morphology near a surface, depending on surface character or starting composition, is discussed.

2. Experimental Section

2.1. Preparation of Two-Dimensional Molds. Glass slides (denoted as G) and Octadecylsilyl- (Octadecyldimethyl chlorosilane-) coated glass slides (denoted as O) were used, respectively, as hydrophilic and hydrophobic plates to construct a two-dimensionally confined space. Each plate was subjected to ultrasonic cleaning in water, followed by rinsing with ethanol and drying in air. Then, the plates were brought together into G–G and O–O pairs with various spacers such as 50 μm , 30 μm , and 13 μm in thicknesses between them as schematically shown in Figure 1. The actual thickness of each gel, which was determined by LSCM, and corresponding spacer will be described in the following section. For LSCM observation, one plate of each mold was replaced by cover glass. In the notation of the molds, an initial letter indicates silicon alkoxides (T for TMOS and M for MTMS), the following number indicates the thickness of the sample, and the following two letters indicate the set of plates. All the molds were placed in an identical polystyrene vessel (the reaction vessel) to be used as a reaction container.

2.2. Preparation of the Starting Solution (MTMS System). First, 15.08 g of 1.0 M aqueous solution of nitric acid and 31.58 g of formamide (FA) as a polar solvent and 0.04 g of fluorescein as a fluorescence dye for LSCM observation were

homogeneously dissolved. Then, 40 mL of MTMS was added under vigorous stirring in an ice-cooled condition. That is, the molar ratio of starting solution was MTMS:FA:H₂O = 1:1.8:2.0. After being stirred for 5 min, the resultant homogeneous solution was transferred into the reaction container followed by 1 min of ultrasonic agitation and 5 s of evacuation with an aspirator to introduce the solution into the molds. The reaction solution was then allowed to gel at 40 °C in a closed condition. The resultant gel was aged at the same temperature for 24 h and then the aged gel (wet gel) was subjected to LSCM. After observation, the gel was dried at 40 °C and the dried monolithic gel was again observed by LSCM. The dried gels are also observed under SEM (S-510, Hitachi Ltd., Japan). Hereafter, we denote the gel prepared between plates as “confined gel” and the bulk gel of the same composition as “monolithic gel”.

2.3. Preparation of the Starting Solution (TMOS System). The preparation procedure is almost the same as the MTMS system described above. The starting composition is as follows: 9.75 g of 1.0 M nitric acid, 33.53 g of formamide, 0.02 g of fluorescein, and 50 mL of TMOS. That is, the molar ratio of starting solution was TMOS:FA:H₂O = 1:2.2:1.5.

2.4. LSCM Observation and Image Processing. The interfacial structure of the resultant gel was observed by LSCM (Carl Zeiss, LSM 510). An oil-immersed 63 \times /1.25 objective lens (Plan-Neofluar, Carl Zeiss) was used. The increment along the z-direction was 0.50 μm for all samples. The resolution in the z-direction is estimated to be approximately 1 μm . The observation direction is along the z-direction as indicated in Figure 1. The laser was scanned in the plane perpendicular to the z-direction (x–y plane), measuring fluorescent intensity in a two-dimensional optically sliced image composed of 512 \times 512 pixel². In the wet confined gel, pores were filled with the solvent containing fluorescein. The Ar laser with 488-nm wavelength was used to excite fluorescein molecules. Dried monolithic gel was observed in almost the same way as reported elsewhere;³⁹ the dried monolithic gel was immersed in a mixture of toluene and chloroform (17:83) to allow the laser light to transmit through the turbid gel, and a 488-nm Ar laser was used to excite fluorescein molecules distributed in the gel phase.

The LSCM images were digitized and 3D reconstructed by stacking the digitized 2D images.³⁸ The depth profiles (along the z-direction) of volume fraction of siloxane phase are depicted by calculating the area of siloxane phase in the series of digitized images for all confined samples. The characteristic lengths of the phase-separated structure are determined by the structure factor $S(q)$; it is obtained from Fast Fourier Transformation of the series of digitized images averaged in the q_x – q_y plane. The interfacial curvatures of the samples were also computed using the Parallel Surface Method and were further scaled with respect to the interfacial area per unit volume. The details of these analyses can be found elsewhere.^{37–39}

3. Results and Discussion

3.1. The Geometrical Properties of the Bulk Gels.

Figure 2 shows the 3D reconstructed images of the dried monoliths of (a) the MTMS system and (b) the TMOS system. The characteristic length determined from the structure factor and the volume fraction of methylsiloxane or silica gel and the area-averaged mean and Gaussian curvatures are listed in Table 1. The area-averaged curvatures $\langle H \rangle$ and $\langle K \rangle$ are scaled by the interfacial area per unit volume Σ , that is, $\langle \tilde{H} \rangle = \langle H \rangle / \Sigma$ and $\langle \tilde{K} \rangle = \langle K \rangle / \Sigma^2$. The characteristic length of the MTMS-derived gel is much longer than that of the TMOS-derived gel, indicating that the spinodal decomposition is frozen in a later stage. These data are in good agreement with results previously reported for sintered co-continuous silica gel: Both the solvent and siloxane phases are co-continuous exhibiting the 3D periodic isotropic structure; the scaled mean and Gaussian curvatures of the dried monolithic gels derived from MTMS and TMOS, respectively, are around zero and negative. This means that most of the interface

(34) Krausch, G.; Dai, C.; Kramer, E. J.; Marko, J. F.; Bates, F. S.; *Macromolecules* **1993**, *26*, 5566.

(35) Kanamori, K.; Ishizuka, N.; Nakanishi, K.; Hirao, K.; Jinnai, H. *J. Sol-Gel Sci. Tech.* **2003**, *26*, 157.

(36) Jinnai, H.; Nishikawa, Y.; Koga, T.; Hashimoto, T. *Macromolecules* **1995**, *28*, 4782.

(37) Jinnai, H.; Koga, T.; Nishikawa, Y.; Hashimoto, T.; Hyde, S. T. *Phys. Rev. Lett.* **1997**, *78*, 2248.

(38) Jinnai, H.; Nishikawa, Y.; Morimoto, H.; Koga, T.; Hashimoto, T. *Langmuir* **2000**, *16*, 4380.

(39) Jinnai, H.; Nakanishi, K.; Nishikawa, Y.; Yamanaka, J.; Hashimoto, T. *Langmuir* **2001**, *17*, 619.

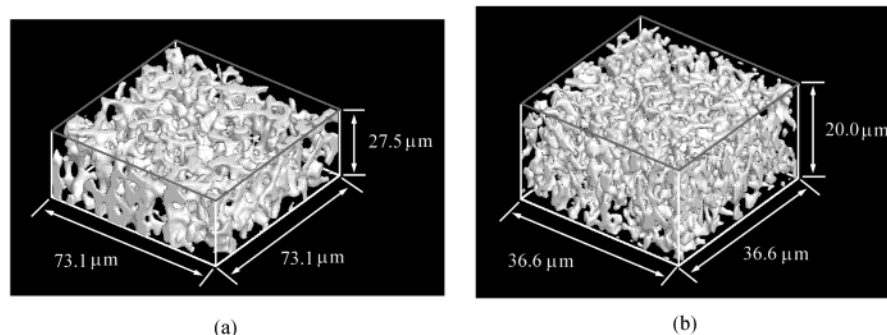


Figure 2. Three-dimensionally reconstructed images and structure factors of (a) dried monolithic gel of the MTMS system and of (b) dried monolithic gel of the TMOS system. Each gel shows the typical co-continuous structure derived from spinodal decomposition.

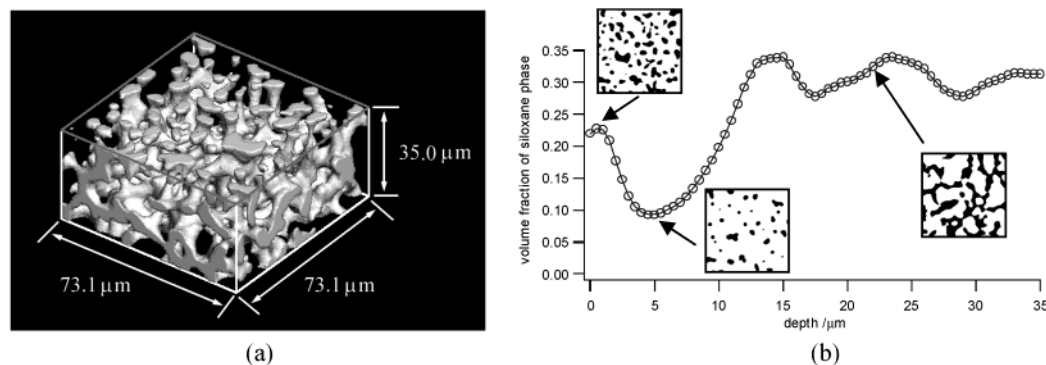


Figure 3. The 3D reconstructed image and the depth vs volume fraction profile of aged M5900. The uppermost plane of the reconstructed image represents the surface ($z = 0$). The columnlike structure that connects the interface and the bulk phase can be seen in upper part of the image.

Table 1. The Characteristic Length, Volume Fraction of Silica or Methylsilicate, the Scaled Mean Curvature, and Gaussian Curvatures of the Dried Monolithic Gels

	characteristic length (μm)	volume fraction of siloxane phase	scaled mean curvature $\langle \bar{H} \rangle$	scaled Gaussian curvature $\langle \bar{K} \rangle$
dried MTMS monolithic gel	14.1	0.25	0.535	-1.61
dried TMOS monolithic gel	3.86	0.22	0.782	-0.836

between the two phases is hyperbolic, which is typical in co-continuous structures induced by spinodal decomposition.³⁹

3.2. Structural Variation near a Hydrophobic Surface. **3.2.1. The MTMS System.** Figure 3 shows the (a) 3D reconstructed image and (b) depth profile of the aged sample M5900, where $z = 0$ indicates the position of the hydrophobic surface. The thickness of the spacer used for M5900 was $30 \mu\text{m}$; however, the actual thicknesses of the synthesized gels were thicker than the thickness of the spacer. This discrepancy of the thickness is thought to be due to the unintended curve of the cover glasses and/or subtle folding of the thin spacers. According to SEM observation, a skin layer has grown at the surface of the methylsiloxane gel film contacting the hydrophobic surface. The skin layer has formed as a result of complete wetting by the methylsiloxane phase on the hydrophobic surface because of the low polarity of the methylsiloxane phase. Since the thickness of the wetting layer is quite thin (approximately a hundred nanometers), it is far below the resolution of LSCM, so a completely accurate profile of the confined gel-hydrophobic surface interface cannot be depicted.

In the thin polymer blend films (approximately tens to hundreds of nanometers thick), when one component segregates preferentially to a surface, surface-directed spinodal decomposition leads to a layered structure (i.e., lamellar structure) perpendicular to the surface. However, in the present system, layered structure appears only at

close proximity to the surface when the sol-gel transition occurs and arrests the phase separation, so it is hard to conclude that the layered structure would develop throughout the film. Nonetheless, because of the complete wetting of the hydrophobic surface, a methylsiloxane depletion layer has formed beneath the skin layer. In the region deeper than the methylsiloxane depletion layer, in the bulk phase, there exists a co-continuous structure, which proceeds into the thick film.

The morphology of the methylsiloxane depletion region appears as cylindrical columns perpendicular to the surface, connecting the skin layer and the bulk phase. The representative digitized sliced images at various positions in the z -direction are inset in Figure 3b; the white and black regions correspond to the solvent and siloxane phases, respectively. The siloxane phase is dispersed in the major solvent phase in the depletion region; in the deeper region, a co-continuous "bulk phase" appears.

3.2.2. The TMOS System. Figure 4 shows the (a) 3D reconstructed image and (b) depth profile of the aged sample T7400 (the thickness of the spacer is $13 \mu\text{m}$). From SEM observation, it is revealed that the skin layer has developed at the interface, as seen in the MTMS system. The surface of TMOS oligomer is generally thought to have hydrophilic character; however, the starting composition of this system contains less than the stoichiometric amount of water for hydration, so the surface of the alkoxy-containing silica gel can be highly hydro-

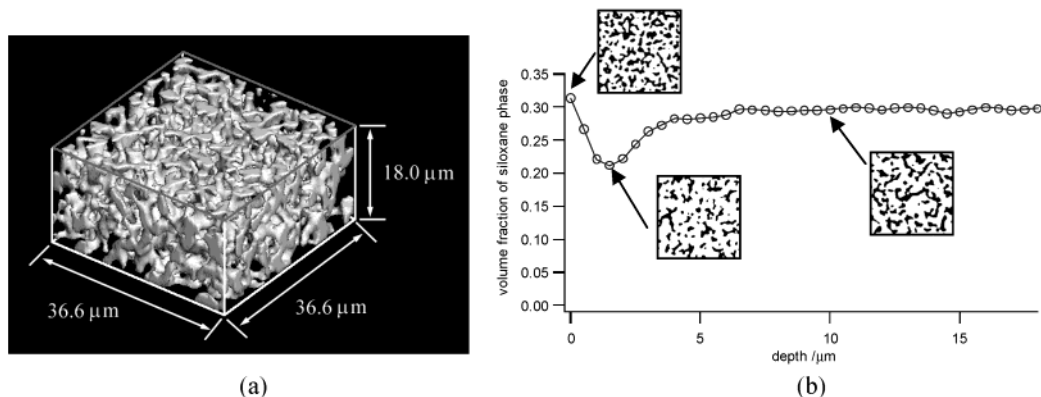


Figure 4. The 3D reconstructed image and the depth vs volume fraction profile of aged T74OO. Unlike the MTMS system, co-continuous structure is maintained throughout the sample.

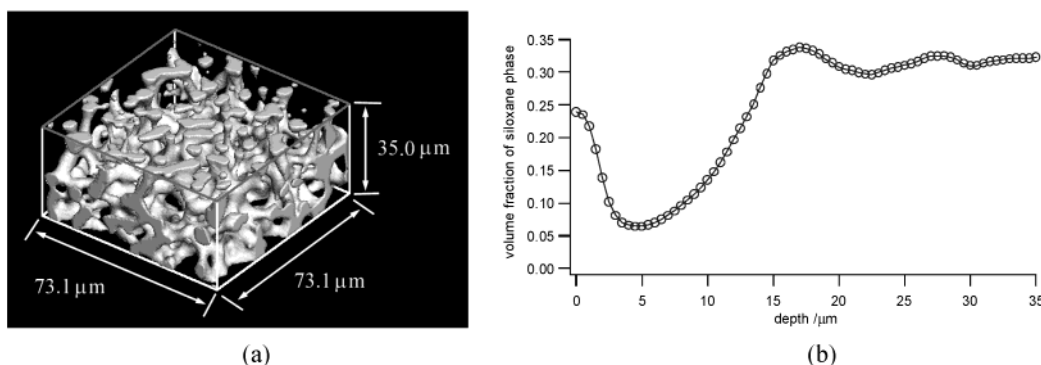


Figure 5. The 3D reconstructed image and the depth vs volume fraction profile of aged M83GG. There is little difference between this case and hydrophobic case (Figure 3), though the adsorption mechanism is quite different.

phobic. For this reason, the morphology and the depth profile are similar to the MTMS system. In this case, however, the depletion is shallower than that of the MTMS system (see Figure 3b).

In the depletion layer of the MTMS system, cylindrical columns connecting the skin layer and the bulk phase have formed, but these cannot be found in the TMOS system. This difference can be explained as follows: Since unreacted silanols in the gel condense during the aging process, the gel shrinks to some extent. The density of the siloxane network is lower in MTMS-derived gel because each monomer has only three functional groups that can react. Therefore, when the gel shrinks toward the center of the film, MTMS-derived gel skeleton is flexible and can stretch to endure the stress of shrinkage, so the cylindrical columns perpendicular to the surface are formed. On the other hand, the siloxane network of TMOS-derived gel is thought to be more rigid than MTMS-derived gel, so the gel skeleton cannot change its shape during shrinkage. Instead, the gel skeleton broke up in the drying process, in which more shrinkage occurs because of the evaporation of the solvent, while MTMS-derived gel did not crack at all. This fact is also confirmed by the inset images in Figure 4b; co-continuous structure is maintained throughout the sample.

3.3. Structural Variation near a Hydrophilic Surface.

3.3.1. The MTMS System. Figure 5 shows the (a) 3D reconstructed image and (b) depth profile of the aged sample M83GG (the thickness of the spacer is 13 μm). In contrast to the hydrophobic surface, the interaction between the hydrophilic surface and MTMS oligomer is thought to be repulsive; however, the depth profile appears similar to the hydrophobic case (see Figure 2b). The MTMS oligomers with low polarity are thought to exhibit a repulsive interaction with hydrophilic surfaces; however,

Si–O–Si chemical bonds can form between the silanol groups on the hydrophilic glass surface and MTMS oligomers or monomers, so a rather attractive interaction between them leads to partial wetting of MTMS phase to the hydrophilic surface. More importantly, the partial wetting forms “footholds” to endure the shrinkage of gel phase that leads to the methylsiloxane depletion layer beneath the surface just as the hydrophobic case. The depth profile looks quite similar to the case of hydrophobic surface. Since the skin layer at the hydrophobic surface is quite thin, it has barely influenced the morphology in the deeper region, which resulted in little difference between hydrophobic and hydrophilic cases.

3.3.2. The TMOS System. Figure 6 shows the (a) 3D reconstructed image and (b) depth profile of the aged sample T82GG (the thickness of the spacer is 30 μm). In this case, as is described above, since the surface character of TMOS oligomer is probably highly hydrophobic, partial wetting by TMOS oligomers could have occurred on a hydrophilic surface, which resulted in almost the same behavior as the MTMS system.

In summary, both kinds of affinity between the gel phase and the surface (either hydrophobic interaction or forming a chemical bond) lead to the gel depletion layer in both alkoxide systems. The surface segregation tendency is thought to be stronger for the hydrophobic interaction, which resulted in complete wetting of the gel phase on the surface. The shape of the gel depletion layer is quite different between the two alkoxide systems because of the difference in cross-linking density.

The characteristic lengths of the co-continuous structures of the confined gels are longer than for the monolithic gels. Although we cannot give an explicit account for this phenomenon at the present stage, it is probable that the

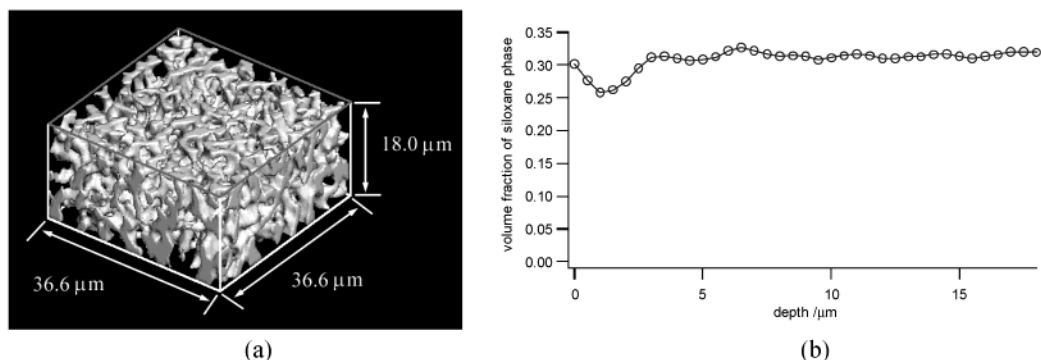


Figure 6. The 3D reconstructed image and the depth vs volume fraction profile of aged T82GG. Again, though the adsorption mechanism is thought to be quite different, there is little difference between this case and the hydrophobic case (Figure 4).

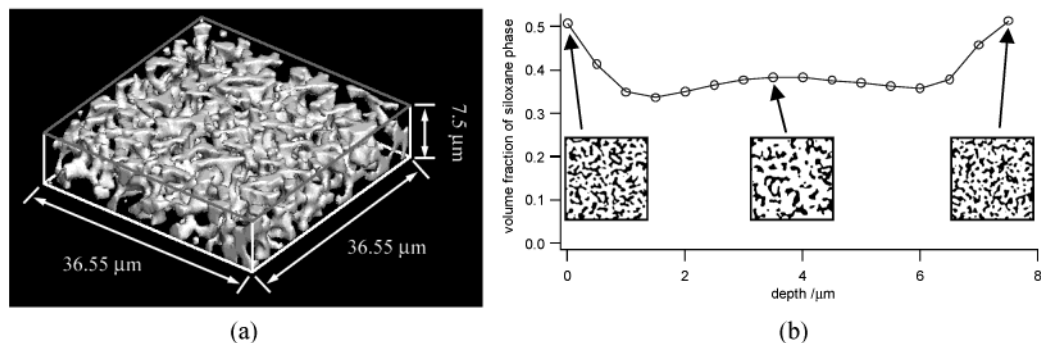


Figure 7. The 3D reconstructed image and the depth vs volume fraction profile of aged T8GG. Interference of spinodal waves from both side of surface is confirmed.

shrinkage during the condensation reaction of silanols is restricted because of the geometrical confinement.

3.4. A Special Case (the Thinner Sample). Figure 7 shows the (a) 3D reconstructed image and (b) depth profile of the thinner sample T8GG (the thickness of the spacer is 13 μm). The film thickness is slightly greater than the spinodal wavelength of the monolithic gel; we can see the oscillating compositional waves penetrating from both sides of the film in the profile, as is seen in thin polymer blend films.³⁴ As compared with the thicker samples, the depletion is shallower indicating that the influence of the opposite surface could reach the depletion region. Besides, the film morphology exhibits co-continuous structure throughout the film, which results in a more homogeneous structure than in the thicker samples.

4. Conclusion

Co-continuous silica-based gels were synthesized in 2D confined spaces and 3D observation was performed by LSCM. The volume fraction of the confined gels oscillates with depth near the surface. The structural variances of

the thicker films near a hydrophobic surface and a hydrophilic surface are similar to each other; however, SEM observation reveals that a skin layer has formed at the interface of a hydrophobic substrate. In the MTMS system, a cylindrical columnar gel skeleton formed in the methylsiloxane depletion region, which reflects the flexibility of the three-functional gel. Conversely, since the TMOS-derived gel has a more rigid siloxane network, such deformation could not occur. In the thinner film, oscillating compositional waves perpendicular to the surface interfere with each other.

Acknowledgment. Financial support by a Grant-in-Aid for Scientific Research from the Ministry of Education, Science, Sports, Culture, and Technology, Japan is gratefully acknowledged. H. J. is partially supported by the Grant-in-Aid for Scientific Research on Priority Areas (A), "Dynamic Control of Strongly Correlated Soft Materials" (No. 413/13031057 & 14045246) from the Ministry of Education, Science, Sports, Culture, and Technology.

LA026715S